The final publication is available at

https://doi.org/10.1016/j.measurement.2022.111340

Additional Information

Fault detection and classification in kinematic chains by means of PCA extraction-reduction of features from thermographic images

Abstract: Kinematic chains are essential elements configurable in different topologies according to the requirements of industry. Their main components are the rotating machines and mechanical parts in which diverse faults can appear. Nowadays, infrared imaging analysis has gained attention for monitoring kinematic chains, however, the approaches for detecting and classifying faults still can be improved. Therefore, this work presents a methodology that uses a low-cost infrared measurement system and combines adequate techniques, such as infrared images preprocessing and segmenting, extraction of statistical indicators, generation of a high-dimensional matrix of features, features reduction, and categorization, for accurately detecting and classifying a wide variety of fault conditions in kinematic chains. This approach was applied to a configurable kinematic chain under the following conditions: healthy motor, misalignment, unbalance, one and two broken rotor bars, bearing faults on the outer race, healthy gearbox, and gearbox wearing. The obtained results validate the effectiveness of the proposed methodology.

1   Introduction

The kinematic chains have been along the time very important elements for a wide variety of processes in the industrial sector, they are used for generating motion though rotating machines. These chains allow to define different configurations among its elements, according to every requirement of the machinery, or a specific process [1]. For example, the actuators in a robot are required for tracking a path. Generally, kinematic chains are integrated by an ensemble of elements such as the induction motor, bearings, pulleys, couplings, and gear boxes [2]. It is very common that at industry the machines integrate multiple kinematic chains making the systems very complex increasing the probability of faults occurrence. Therefore, due to the number of elements that compose a chain, and its complexity, make them systems susceptible to suffer a great variety of failures, under different origins. That is the reason for which its study/monitoring for fault diagnosis is still the focus of interest for a diverse amount of research.

The monitoring of faults in the kinematic chains, of the machines and industrial processes, allows to increase their efficiency, to rise the productivity, to extend their lifespan, as well as to reduce their maintenance costs [3]. Among the most common faults taking place into a kinematic chain are the following: coupling misalignments, unbalance in transmission pulleys, wearing and breakage of rolling bearings, wear and tear of gearboxes, and faults in the induction motor. In turn, the most common faults in motors are the following: broken rotor bars, bearing wear, winding short circuits, among others [4]. All these faults can affect

the overall efficiency of the chain in the processes manifesting them as heat released. The importance of keeping the kinematic chains operating continuously without anomalies has triggered the development and usage of new noninvasive methodologies for faults detection.

Among the different methodologies reported for monitoring fault conditions in electromechanical systems that typically integrate a kinematic chain, the most common are those based on data acquisition from physical variables and further signals processing. Some examples of such approaches are the motor current signature analysis (MCSA) [5 - 6], mechanic/acoustic vibrations analysis [7 - 8], and temperature analysis [9 - 11]. Also, there exist works where statistical parameters and artificial intelligence techniques are used [12]. However, some aspects are still not being explored like performance improvement in the data processing, hybridization of techniques, utilization of more efficient low-cost noninvasive sensors, integration of the system as all-in-one package, etc. In the last years the usage of thermographic analysis has been addressed with growing interest on various elements from a kinematic chain [10]. This can be attributed to the advantages provided by this technology, since it offers an alternative noninvasive solution for faults detection. Nonetheless, some drawbacks were present at the beginning in the usage of thermography: the infrared sensors, or infrared cameras, were commercial closed systems that used to make the monitoring systems as high-cost solutions that needed to be calibrated. Also, additional elements were required to validate the calibration process, such as external temperature sensors, for instance, the thermocouples [10 - 13]. So that, until some years ago thermography had been used as complementary tool of other techniques. The relevance of the thermography has been reported recently in the field of faults diagnosing in rotating electric machines at industry, and this is demonstrated in several works from which it has been addressed the processing of infrared images for detecting and classifying specific faults, for example in diagnosing bearing faults [14 – 19]. Also, the infrared images processing has been used for detecting faults in a cooling radiator [20]. All these works demonstrate that faults detection can be affectively performed through thermographic analysis for a specific element into a system, it would be desirable, as well, to detect faults in several elements of the system; even considering a combination of adequate techniques such as features extraction, intelligent algorithms, deep learning, classifiers, etc., for achieving this task.

Nowadays, thanks to the development of low-cost automatic self-calibration infrared cameras, the thermographic analysis has been consolidating as an independent methodology for monitoring faults in electromechanical systems [21]. These new thermographic devices can acquire infrared signals from elements in a process and allow finding heat points related to the faults conditions inside the system [22]. The topic of thermographic images analysis for detecting faults in single components of an electromechanical system has been tackled by many scientific researchers, by using a variety of image processing and machine learning techniques [23]. For example, in [24] were presented five study cases about the feasibility of using infrared-thermography technology to give support in methodologies for detecting faults in induction motors. In this work, the authors reported different motor-related faults, such as: cooling fault, rolling bearing lubrication fault, and connections and windings in faulty state. By its part, in [25] was implemented the Otsu's algorithm for segmenting the thermographic images from a kinematic chain and thus, calculate the temperature difference to make the comparison of the chain state. Additionally, this work reported four types of faults: healthy state, broken rotor bars faults, rolling bearing faults, and misalignment faults. In this regard,

the research presented in [26] presents the analysis and classification of thermographic images by means of decision trees (DT) for a diagnosis system of electric machines, transformers and induction motors. Their proposed approach considers 11 gradual states of electric short-circuit faults and it allows to obtain predictions with an accuracy up to 93.8% in the diagnosis. Another work that develops a methodology for automatic detection of faults in rolling bearings is presented in [27]. In that work, a 2-dimensional discrete wavelet transform (2D-DWT) is applied to the thermographic images followed by the extraction and reduction of statistical features. Additionally, with the help of a support vector machine (SVM) it is classified the bearing state, reaching a 97% of accuracy in the prediction. In other approach, an automatic segmentation of thermographic images over the region of interest of a kinematic chain was performed by applying the scale invariant feature transform (SIFT) [28]. This process was performed along with the Naives-Bayes classifier to automatically detect rolling bearings faults, broken rotor bars, and motor fan faults with an accuracy in the diagnostic reported of 100%. In this same line the work presented by [29] demonstrates the flexibility and robustness of the thermographic analysis when the regions of interest are obtained by SIFT for further features extraction through a previously trained neural network. In this work the classification task is made by the SVM. The validation is made considering only electric fault conditions in an induction motor. Even though, the reported techniques in the literature have addressed the monitoring of fault conditions in electromechanical systems their results can be improved if adequate techniques are selected individually or combined, not to mention that just some faults are reported, typically 5 to 6, in average. It would be interesting to develop a methodology capable of handling most of the reported faults, not only in induction motors but also in kinematic chains integrated in the industrial processes.

The contribution of this work is a methodology that combines adequate techniques with a proprietary system for detecting and classifying fault conditions in a configurable kinematic chain, considering not only the rotating machine but also other elements in the chain and thus handling a wide variety of possible fault conditions, mechanical and electrical. The methodology starts with the acquisition of the infrared images from the kinematic chain, made through a low-cost infrared camera connected to a commercial microcontroller unit (MCU). The implemented algorithms enable the system to use the infrared camera in less restricted positions, unlike the commercial systems. The infrared images captured are preprocessed by the Otsu's algorithm for reducing the background noise. Then, the points of interest from the kinematic chain are obtained by applying the SIFT algorithm on the image to yield an adequate region of interest (ROI). These regions are helpful for generating a histogram from which statistical indicators are calculated. The indicators, in turn, are used to generate a high dimensional matrix of features that contains non-visible information about data behavior associated to the fault conditions in the chain. In order to find out those features that are most helpful for detecting the fault conditions, a dimensionality reduction of features is performed by means of PCA, this helps to maximize the separation among the conditions detected. Finally, the reduced features feed an artificial neural network (ANN) to perform the classification task allowing a corresponding accuracy above the 96% in the diagnosis. Whereas other works handle some faults, in this approach a total of 12 faults are considered, which are grouped as follows: healthy condition, unbalance, misalignment, broken rotor bars, rolling bearing faults, and gearbox faults. The results obtained validate the efficiency of the proposed approach for detecting and classifying different fault conditions in rotating machines and their associated components.

3

2 Theoretical Background

2.1 Image Segmentation

One of the classic methods for image segmentation is Otsu's algorithm [30]. This method uses an automatic algorithm to eliminate the background of an image by dividing the histogram in two classes C_0 and C_1 separated by a threshold value, k. The best value of k is the one that maximize the inter class variance expressed by σ_b^2 in (1):

$$\sigma_b^2(k) = \omega_0(k)\omega_1(k)[\mu_0(k) - \mu_1(k)]^2 \tag{1}$$

$$\omega_0(k) = \sum_{i=0}^{k-1} p(i) \tag{2}$$

$$\omega_1(k) = \sum_{i=k}^{L-1} p(i) \tag{3}$$

$$\mu_0(k) = \frac{\sum_{i=0}^{k-1} k \cdot p(i)}{\omega_0(k)} \tag{4}$$

$$\mu_1(k) = \frac{\sum_{i=k}^{L-1} k \cdot p(i)}{\omega_1(k)} \tag{5}$$

Where $\omega_{0,1}$ is the probability function on class C_0 (2) and C_1 (3), $\mu_{0,1}$ is the mean value of class C_0 (4) and C_1 (5), L is the number of gray levels in the image, and p is the probability of any given pixel to be in a gray level.

2.2 Scale Invariant Feature Transformation (SIFT)

Lowe's method [31], commonly known as SIFT (Scale Invariant Feature Transform), for the extraction of scale invariant key points is one of the most effective algorithms for the localization and segmentation of objects in an image [32]. The method follows four main steps:

1) *Scale-space extrema detection*: The scale-space of an image is calculated using (6) for the difference of Gaussian functions to identify potential points invariant to rotation and scale.

$$D(x, y, \sigma) = G(x, y, k\sigma) * I(x, y) - G(x, y, \sigma) * I(x, y) \tag{6}$$

Where *I(x, y)* is the original image, and σ is the scale or standard deviation for the Gaussian function *G(x, y, σ)* convoluted with the image *I*.

2) *Key point localization*: Each potential key point is evaluated by an edge-detection and low-contrast model to keep only those key points with more stability in the image.

3) *Orientation assignment*: An orientation is assigned to each key point based on the local gradient properties of the image in order to improve the invariant nature of the key points to

4

scale and rotation, the gradient properties, m and θ are calculated using (7) and (8) respectively:

$$m = \sqrt{\left(I(x,y) - I(x+1,y)\right)^2 + \left(I(x,y) - I(x,y+1)\right)^2} \tag{7}$$

$$\theta = \tan^{-1}\left[\frac{I(x,y) - I(x,y+1)}{I(x,y) - I(x+1,y)}\right] \tag{8}$$

2.3 Histogram characteristics

The histogram of a thermal image describes the distribution of pixels in a defined number of grey levels. It is possible to extract different statistical characteristics that can be used to condense the information available in a thermal image [33]. Equations (9) to (23) of Table 1 describe the statistical characteristics that were chosen for this system: mean, maximum value, root mean square (RMS), square mean root (SMR), standard deviation, variance, form factor with RMS, form factor with SMR, crest factor, latitude factor, impulse factor, skewness, kurtosis, 5th moment, and 6th moment.

Table 1. Histogram statistical indicators defined.

Indicator	Equation	
Mean	$T_1 = \dfrac{\sum_{n=1}^{N} h(n)}{N}$	(9)
Maximum value	$T_2 = \max\lvert h(n)\rvert$	(10)
Root Mean Square (RMS)	$T_3 = \sqrt{\dfrac{\sum_{n-1}^{N}\left(h(n)\right)^2}{N}}$	(11)
Square Mean Root (SMR)	$T_4 = \left(\dfrac{\sum_{n=1}^{N}\sqrt{\lvert h(n)\rvert}}{N}\right)^2$	(12)
Standard Deviation	$T_5 = \sqrt{\dfrac{\sum_{n=1}^{N}(h(n) - T_1)^2}{N-1}}$	(13)
Variance	$T_6 = \dfrac{\sum_{n=1}^{N}(h(n) - T_1)^2}{N-1}$	(14)
Form Factor with RMS	$T_7 = \dfrac{T_3}{\frac{1}{N}\sum_{n=1}^{N}\lvert h(n)\rvert}$	(15)
Form Factor with SMR	$T_8 = \dfrac{T_4}{\frac{1}{N}\sum_{n=1}^{N}\lvert h(n)\rvert}$	(16)
Crest Factor	$T_9 = \dfrac{T_2}{T_3}$	(17)
Latitude Factor	$T_{10} = \dfrac{T_2}{T_4}$	(18)
Impulse Factor	$T_{11} = \dfrac{T_2}{\frac{1}{N}\sum_{n=1}^{N}\lvert h(n)\rvert}$	(19)
Skewness	$T_{12} = \dfrac{1}{N}\cdot\dfrac{\sum_{n=1}^{N}(h(n) - T_1)^3}{T_5^3}$	(20)
Kurtosis	$T_{13} = \dfrac{1}{N}\cdot\dfrac{\sum_{n=1}^{N}(h(n) - T_1)^4}{T_5^4}$	(21)
5th Moment	$T_{14} = \dfrac{1}{N}\cdot\dfrac{\sum_{n=1}^{N}(h(n) - T_1)^5}{T_5^5}$	(22)

| 6th Moment | $T_{15} = \dfrac{1}{N} \cdot \dfrac{\sum_{n=1}^{N}(h(n) - T_1)^6}{T_5^6}$ | (23) |

The histogram of an image can also be interpreted as a discrete probability distribution or as a discrete signal, which simplify the calculations required to obtain all the previously defined statistical characteristics. The histogram function is called *h(n)* where *n=1, 2, ..., N*. *N* is the total number of different grey levels on the histogram function.

2.4   Principal Component Analysis (PCA)

Principal Component Analysis (PCA) is a mathematical tool used in modern data analysis for different applications such as dimensionality reduction, feature extraction, or data compression. The main objective of this tool is to find the most meaningful representation of a data set [34].

The implementation described here is focused on a dimensionality reduction application of the PCA method. The data to be analyzed with the PCA tool needs to be prepared beforehand considering the following [35]:

- Organize and categorize the raw data to be analyzed in a $n \times p$ matrix, **B**;
- Remove any missing value from the data;
- Associate a numeric value to each qualitative variable in the data;
- Standardize the numeric data (i.e., rescale the data to have a mean of 0 and a standard deviation of 1).

Let the matrix **B** of size $n \times p$ where *n* is the number of samples and *p* is the number of dimensions or variables in the original data, a covariance matrix *C* of size $p \times p$ is calculated using (24):

$$ \mathbf{C} = \frac{1}{n-1} \mathbf{B}^{\mathrm{T}} \cdot \mathbf{B} \tag{24} $$

Where $\mathbf{B}^{\mathrm{T}}$ is the conjugate transpose of matrix **B** for the case of a real matrix. The next step is to calculate the eigenvectors **D** and eigenvalues of matrix **C** through (25):

$$ \mathbf{D} = \mathbf{V}^{-1}\mathbf{CV} \tag{25} $$

Where **D** is a diagonal matrix of size $p \times p$ filled with the eigenvalues of **C** and **V**, with size $p \times p$, is filled with the eigenvectors of **C.**

3   Proposed Methodology

In this section is described the proposed methodology for detecting fault conditions in different elements and configurations of a kinematic chain based on thermography, assuming the chains as series of essential parts for industrial processes. The Figure 1 depicts the general

block diagram of the proposed approach from which three main blocks can be observed as: kinematic chain configurations, thermographic images acquisition, and detection and classification of fault conditions in the kinematic chain.
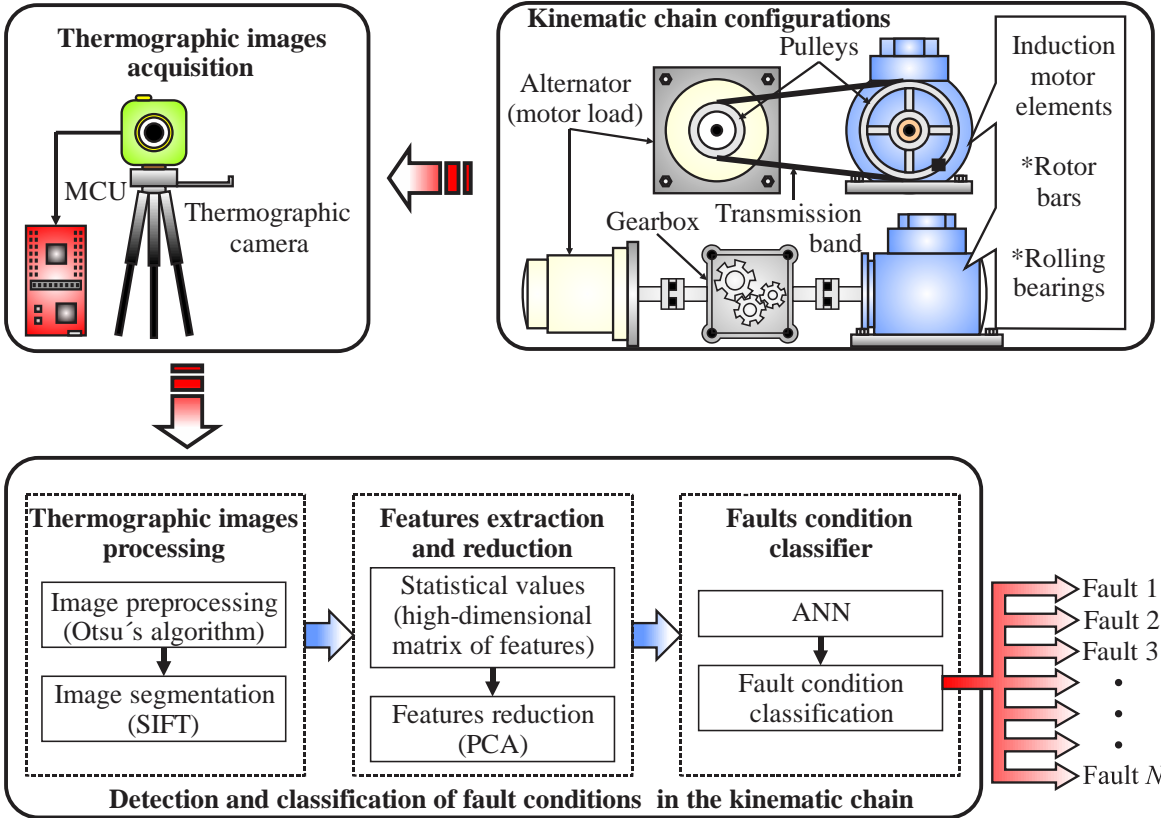
Figure. 1. General block diagram of the proposed methodology for detecting and classifying faults conditions in a configurable kinematic chain.

The first block describes a configurable kinematic chain with the elements that allow to define different connection topologies according to what is required to be analyzed. The elements considered in this work are a three-phase induction motor, an alternator (as a motor load), a gearbox, output shaft pulleys, mechanical couplings, and a transmission band. In such a way that, if particular specifications for the kinematic chain are established, then, the electromechanical elements can be assembled in that particular topology as needed. For instance, the elements in the kinematic chain could be the coupling between the induction motor and the alternator though pulleys and the transmission band, or the coupling between the induction motor and the gearbox through mechanical coupling and rolling bearings. The main idea is to have a methodology able for analyzing several fault conditions no matter the topology of the kinematic chain: since the healthy conditions of the induction motor and the gearbox, to other present faults, such as, broken rotor bars and faults in the rolling bearings inside the motor, wear and tear of gearbox, unbalance on the pulleys, and coupling motor-alternator/gearbox misalignment, among others. It worth to mention that unlike other reported approaches, where just 4 to 6 fault conditions are handled, this work allows to diagnose a wider variety of fault conditions in the whole ensemble. A detailed explanation about the fault conditions for the study cases considered in this work is given in the

experimental setup.

The second block of the proposed methodology consist in the infrared images acquisition during the kinematic chain operation, since anomalies are accompanied by the release of heat. For this task, it is used an infrared camera that acquires a set of thermographic images and store them into an SD card by means of a commercial microcontroller unit (MCU) from Texas Instruments. This set of images is stored from the respective configuration of the kinematic chain. As it will be explained next, the techniques used for processing the images provide the system with the capability of using this nonintrusive infrared camera in a nonrestricted position around the kinematic chain, unlike other works where the position of the camera plays a key role for the success of the diagnosis.

Finally, the third block of the proprietary system consist in detecting and classifying fault conditions on the configurable kinematic chain. To meet this goal, three substages need to be accomplished, to know: thermographic images processing, features extraction and reduction, and faults condition classifier. Firstly, once the thermographic images are sent to a processing unit, they are preprocessed by the Otsu's algorithm for eliminating all the regions that are not considered for analysis (unnecessary background and noise). Thereafter, the points of interest are defined by means of the SIFT technique, which yields a region of interest (ROI) of the image for data processing. Secondly, having defined a ROI, the image histogram is calculated, and it is used to compute the statistical indicators according to expressions (9) to (23) of Table I yielding a lot of values that from now are going to be known as features. These values are used to construct a matrix that will have high dimensionality because of the number of features defined and this arrangement is necessary for the next processing step. The matrix of features is helpful to provide the non-visible information required to detect the fault conditions, since the features could be associated to them. However, some features provide repeated or nonvaluable information and, therefore, it is necessary to discriminate from the features those useful ones, which brings as consequence a reduction in the matrix dimensionality. The aforementioned task is performed through the PCA technique, since it reduces the high-dimensional matrix of features into a 3-dimensional representation of features that shows graphically the conditions detected in the chain as clusters. The objective of the PCA is to reduce the dimensionality of the matrix by maximizing the separation between the classes detected (fault conditions) and to simplify the categorization task by yielding a reduced number of inputs for the classifier. Thirdly, and as last substage, a simple architecture of an artificial neural network (ANN) is used to classify the fault conditions, as consequence of the obtained outputs by the PCA. In this stage, the reduced features computed by means of the PCA are feed to the network as the inputs for training and validation. As last, but not least, the output of the proposed methodology provides the information about the presence of the fault conditions detected in the configuration of the kinematic chain, Fault 1, …, Fault N, according to the information included in the matrix of features.

4   Experimentation

4.1   Experimental setup

The set of experiments were carried out by using a configurable kinematic chain as shown in Figure 2. This kinematic chain can be ensembled in two main topologies: a) motor-

alternator, and b) motor-gearbox. For the motor-alternator configuration, an induction motor, two output shaft pulleys, an alternator acting as motor load, and a transmission band are used. Meanwhile, for the motor-gearbox configuration, the induction motor, the gear box, the alternator, and mechanical couplings are the main components. The electric machine used in both configurations consist in a WEG 3F A.E. 00136AP3E48TCT model induction motor, having a rated power of 0.74 kW, a nominal speed of 3355 RPM, and it is fed with 210-230/460 Vac at 60 Hz. For the motor and the gearbox, two automotive alternators are used as mechanical loads entailing approximately a 10% of the motor load. Meantime, the gearbox model is a Baldor GCF4X01AA with reduction ratio 4:1 driving the motor shaft. By its part, from Figure 2, the c) proprietary thermographic system consists of both the infrared camera and a commercial MCU. The sensor is a low-cost and high-resolution automatic self-calibration infrared micro-camera model FLIR LEPTON 3, located at 0.8 m away from the kinematic chain. The resolution of the obtained image is a 160 x 120 progressive exploration matrix with pixel size of 12 µm. It is a low-cost thermal sensor that can have flexible applications in industrial environments because is not limited by the requirements of space and location, unlike commercial equipment do. Thus, the thermographic images are acquired and stored by the MCU which consist in a platform Raspberry PI 3 by using an SD card of 32 GB. Then the images are sent to the PC.
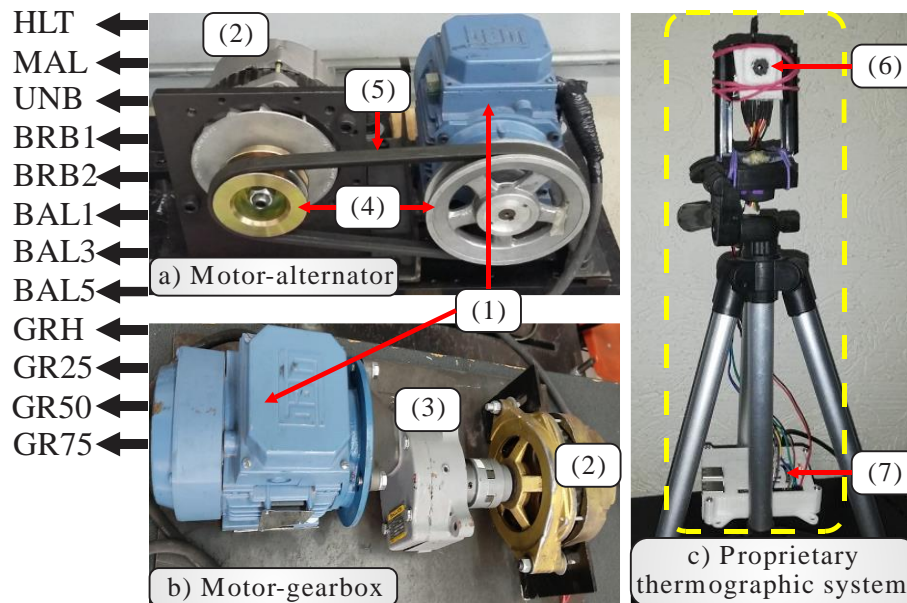
Figure 2. Experimental setup of the kinematic chains configurations a) motor-alternator, b) motor-gearbox, and the c) proprietary thermographic system. The included elements are: (1) induction motor, (2) alternator as motor load, (3) gearbox, (4) output shaft pulleys, (5) Transmission band, (6) low-cost automatic self-calibration infrared camera, and (7) proprietary system based on commercial MCU

4.2 Study cases: fault conditions

The fault conditions considered in this work are described in Table 2 and they are shown in Figure 3. As it can be observed, the fault conditions are taken into account in accordance with the topology configured in the kinematic chain: motor-alternator and motor-gearbox.

Table 2. Fault conditions handled.

| Fault condition	Description	Topology
HLT	Healthy condition of the induction motor	Motor-alternator
MAL	Misalignment between the induction motor and the alternator	Motor-alternator
UNB	Unbalance on the pulley coupled in the induction motor shaft	Motor-alternator
1BRB	1 broken bar into the induction motor case	Motor-alternator
2BRB	2 broken bars into the induction motor case	Motor-alternator
BAL1	Rolling bearing fault on the outer race, with a hole of 1 mm diameter	Motor-alternator
BAL3	Rolling bearing fault on the outer race, with a hole of 3 mm diameter	Motor-alternator
BAL5	Rolling bearing fault on the outer race, with a hole of 5 mm diameter	Motor-alternator
GRH	Healthy condition of the gearbox with not wear or tear	Motor-gearbox
GR25	Wear and tear in the gearbox entailing a 25% of backlash	Motor-gearbox
GR50	Wear and tear in the gearbox entailing a 50% of backlash	Motor-gearbox
GR75	Wear and tear in the gearbox entailing a 75% of backlash	Motor-gearbox

From Table 2 and Figure 3 the fault conditions are simulated as follows. The HLT condition consist naturally in the induction motor and the kinematic chain with all the elements without faults, no misalignment and no unbalance are presented in the couplings. The MAL condition consist in a slight shift between the pulleys of the motor and the load (alternator). Having a top view of the coupling motor-alternator, this shift is achieved by placing the motor approximately 2 cm behind the alternator respect to the horizontal line observed in the figure. In relation to the UNB condition this is achieved by placing a slight mass in the motor pulley, which consist in a screw screwed into the pulley. By its part, the 1BRB consist in a hole of 3mm diameter drilled on one rotor bar, and respectively, the 2BRB condition consist in two holes of 3mm diameter drilled on two rotor bars. In both cases the holes are of 1mm depth. Next, the BAL1, BAL3, and BAL5 conditions are simulated by drilling holes of 1mm depth in three rolling bearings in their outer race, the first one with a 1mm diameter, the second one with a 3 mm diameter, and the third one with a 5 mm diameter, respectively. On the other hand, the GRH condition consist simply by the gearbox without wearing. Finally, the GR25, GR50, and GR75 conditions are simulated by using three gears, the first one with slight tooth wearing, approximately in a 25%, the second one with moderate tooth wearing, approximately in a 50%, and the third one with severe tooth wearing, approximately in a 75%, respectively.

The experimental trials were carried out per fault condition along 90 minutes each one during the kinematic chain operation, and the thermographic images are captured every 10 seconds. However, only the steady state of the system is considered (once the temperature of the kinematic chain has raised), taking only the last 30 minutes and generating 180 images per fault condition. In the image processing stage, the original resolution of the captured images is scaled up to a 520 x 390 matrix by bilinear interpolation.

Next, the matrix of features is structured as illustrated in Figure 4 and reduced by the PCA into a 3-dimensional representation that feeds an ANN for the classification of faults. The structure of the ANN consists in one input layer with 3 neurons, 3 hidden layers with 3, 6 and 12 neurons, respectively, and one output layer with 12 neurons. The activation functions were, hyperbolic for the hidden layers and linear for the output layer. Finally, from the 180 images, 126 were used for training and 54 for validation, defining a 70/30 percentage ratio.
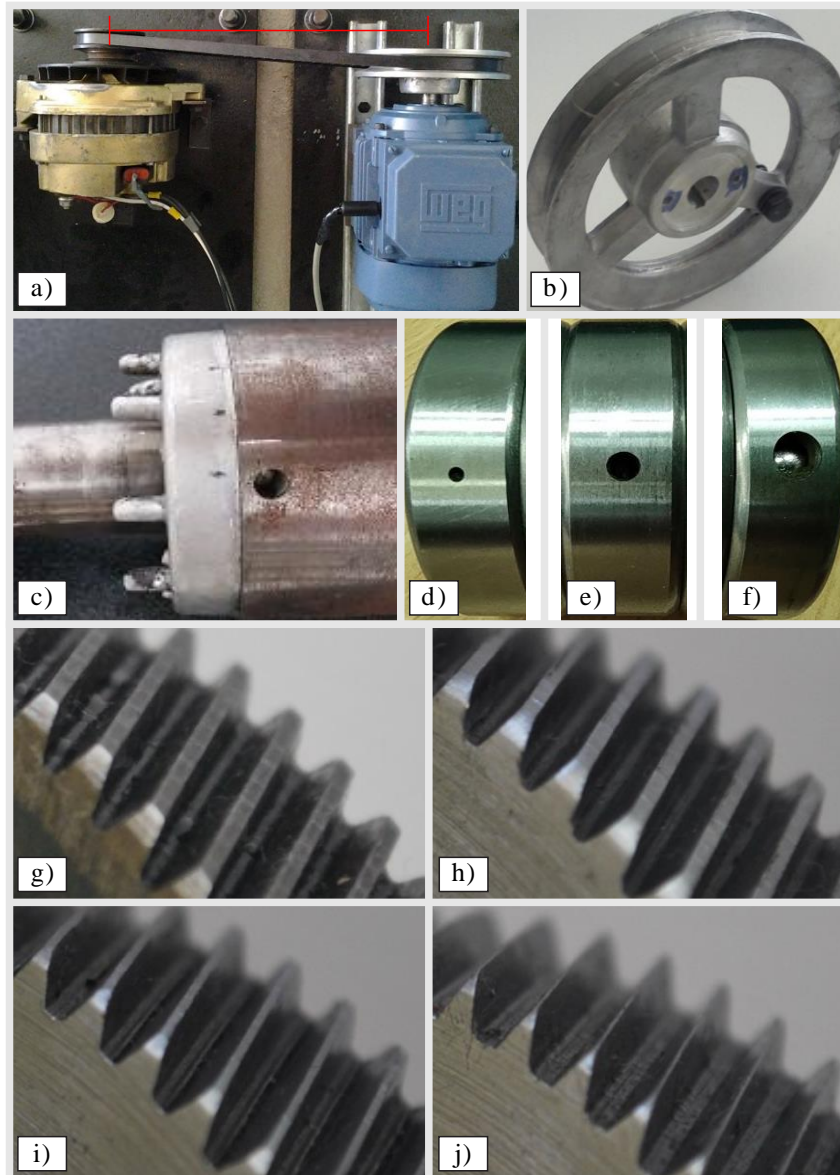
Figure 3. Fault conditions for the motor-alternator, such as a) MAL, b) UNB, c) 1BRB/2BRB, d) BAL1, e) BAL3, f) BAL5, and fault conditions for the motor-gearbox, such as g) GRH, h) GR25, i) GR50, and j) GR75.
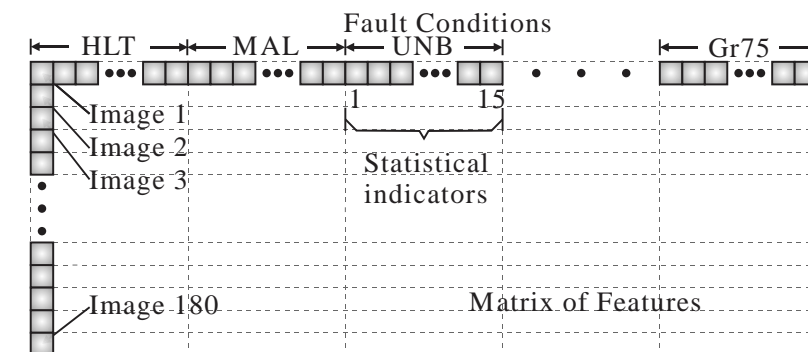

Figure 4. Structure of the matrix of features extracted from the thermographic images.

5   Results

For the obtained results, the Figure 5 a) displays an example of a thermographic image captured directly from the configurable kinematic chain, in this case from the motor-alternator. As previously mentioned, if there exist fault conditions, they come up with an associated increasing of temperature during the chain operation. Once the image is acquired by the MCU, stored, and sent to the PC, it is resized as explained in the previous section. In this point, the Figure 5 b) shows the resulting image when the Otsu's algorithm is applied, remembering that is in charge of clean the image background and eliminates the inherent noise added, that means an image binarization. Next, the points of interest defined by applying the SIFT algorithm (which is used for defining the zone over the image that is going to be analyzed) are observed in Figure 5 c), that is, the ROI. Finally, in Figure 5 d) it is observed the ROI yielded by the image processing, that represent the motor regions isolated to be analyzed.

By means of the ROI the histograms of the images can be computed, two examples are appreciated in Figure 6 a) for a healthy condition and in Figure 6 b) for the 1BRB fault condition.
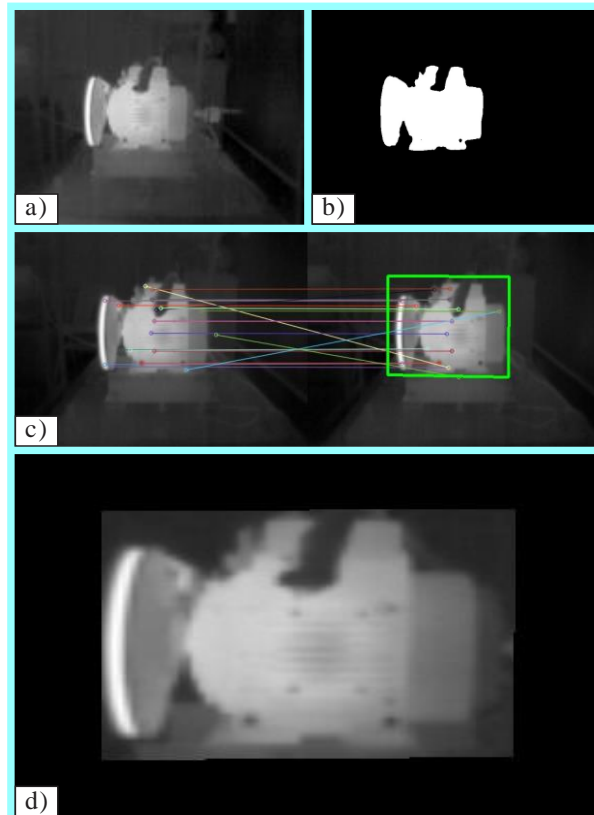

Figure 5. Thermographic preprocessing and processing, in a) original image obtained by the FLIR LEPTON 3, in b) implementation of the Otsu's algorithm, in c) application of SIFT, and d) final ROI for analysis.

After this, the statistical indicators are computed through (9) to (23) from the images' histograms, and the obtained values are structured to generate a high dimensional matrix of features for the 12 fault conditions, as indicated in Figure 4. As a matter of fact, in Figure 7

is presented the reduction performed by the PCA over the matrix of features. From this figure it can be noticed that the fault conditions detected are plotted as clusters into a three-dimensional representation.
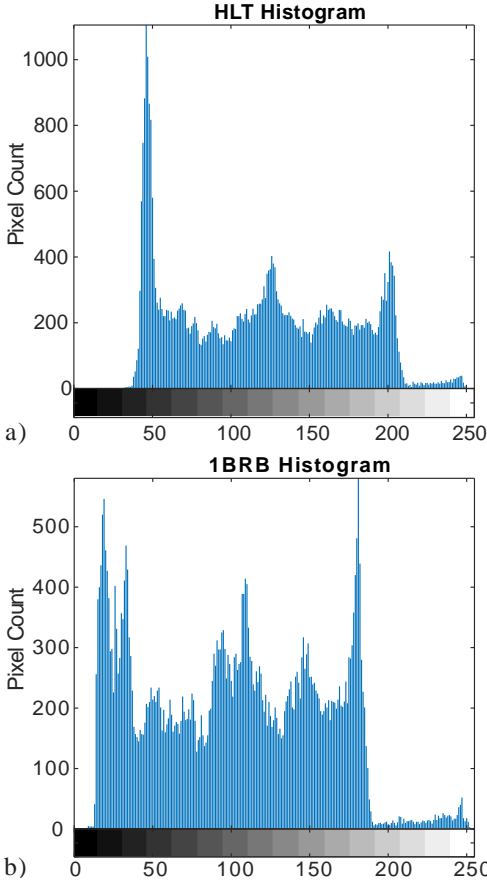
Figure 6. Histograms from the ROI of the example images, in a) for a healthy condition, and in b) for the 1BRB fault condition.
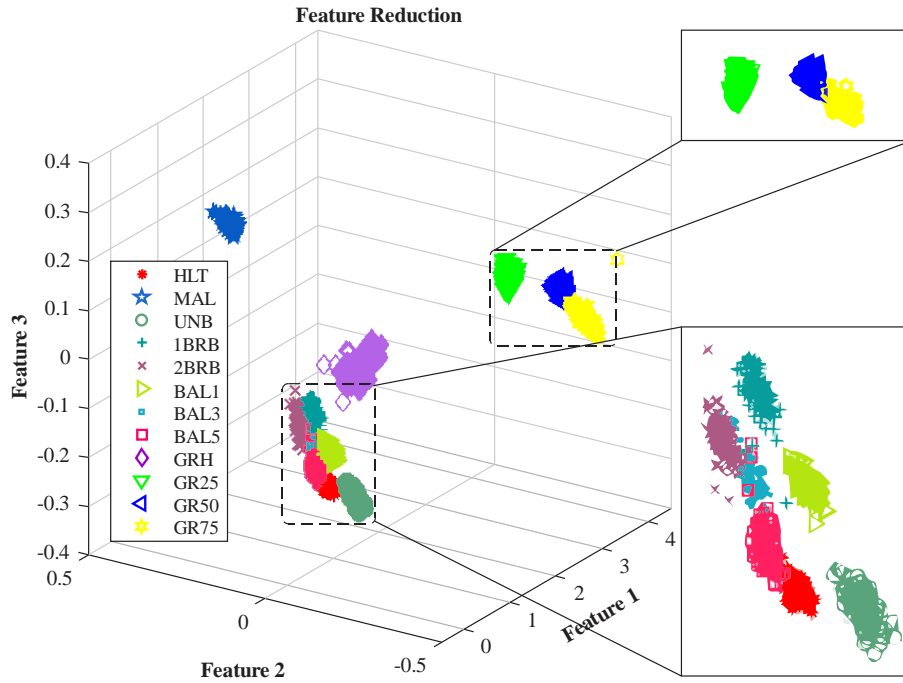
Figure 7. Dimensionality reduction of the matrix of features by applying PCA and 3-dimensional representation of the fault conditions detected as clusters.

Finally, the Figure 8 shows the confusion matrix attained during the classification task by the ANN considering all the 12 fault conditions.

Figure 8. Confusion matrix for the 12 fault conditions classified by the ANN.

6   Discussion

The kinematic chains represent essential elements into the industrial processes, as integral parts of the machines, where motion interchange is required and for that reason it is important the development of noninvasive methodologies for diagnose fault conditions. The obtained results demonstrate the robustness and reliability of the proposed strategy. For example, Figure 5 (a) - (b) shows that the images preprocessing is effective, since the inherent noise of the images is eliminated, and the unnecessary background is completely removed yielding useful binarized images of the kinematic chain through the threshold stablished by the Otsu's algorithm. Also, Figure 5 c) and d) indicates that the SIFT defines adequate points of interest for the images, that means, the ROI is successfully obtained. It worth to mention that any anomaly presented in the kinematic chain will come with an energy change (temperature rising), and hence it will be presented in the ROI. Therefore, the importance of generating a suitable ROI is highlighted when the histogram obtained from this region can provide useful information of the implicit fault condition, but only if the ROI is adequately isolated. Thus, for example, the matrix of features generated through the statistical indicators computed from the histograms will contain useful values that describe the fault conditions into the kinematic chain, however, it is not visible until this matrix is reduced by the PCA. Then, as observed in Figure 7, the reduction of the matrix generates a three-dimensional representation by plotting a cluster for every one of the 12 fault conditions. Finally, the proposed strategy is validated through the ANN-based classifier, which reach a global accuracy up to the 96.8%. In summary, from Figure 8 the fault conditions 2BRB, BAL3, BAL5, GR50, and GR75 are diagnosed with accuracies of 96.3%, 96.3%, 81.5%, 98.1%, and 88.9%, respectively. In contrast, the rest of the conditions reaches the 100% of accuracy in the diagnosis.

7   Conclusions

Since many industrial processes use a wide variety of machines that typically ensemble kinematic chains for generating motion interchange, it is important the diagnostics of the chain elements in order to keep the efficiency as high as possible. This work develops a methodology for monitoring fault conditions in a configurable kinematic chain. It worth to notice that the proposed approach contributes starting with the thermographic proprietary system. For example, an adequate capturing of a thermographic image is essential. It was demonstrated that anomalies in the kinematic chain could affect its efficiency reflecting it as an energy change, like heat released, that could be observed in the thermographic images. In this sense the high-resolution infrared sensor used possess characteristics that enable it for being integrated in a digital system with automatic self-calibration of temperature, which means that not external temperature sensors are required. With all certain, the algorithms implemented for preprocessing and processing the thermographic images plays a key role, for instance, one remarkable advantage of the system is that the location of the camera is not as limited as conventional infrared cameras have. Of course, similar results could be obtained by using a commercial equipment, since the main contribution of this work is the combination of the adopted techniques, but such results would be limited by the characteristic and limitations of the commercial camera. Also, the image processing enhances the proposed strategy to get results of 96.8% as the global accuracy in the final diagnosis demonstrate. On the other hand, the extraction and reduction of statistical features through PCA has

demonstrated that the fault conditions can be clearly detected and visualized as clusters into a three-dimensional representation. With this, it is possible to classify the conditions with a simple structure of the ANN. In future work, other signals from additional sensors would be added to the proposed methodology in order to explore if the accuracy can be raised. Also, other different configurations of the kinematic chain and more fault conditions will be considered an analyzed.

8   References

[1] C. Liu. (2018). Emerging Electric Machines and Drives — An Overview. *IEEE Transactions on Energy Conversion*, vol. 33, no. 4, pp. 2270-2280, https://doi.org/10.1109/TEC.2018.2852732

[2] A. G. Garcia-Ramirez, L. A. Morales-Hernandez, R. A. Osornio-Rios, J. P. Benitez-Rangel, A. Garcia-Perez, and R. D. J. Romero-Troncoso. (2014). Fault detection in induction motors and the impact on the kinematic chain through thermographic analysis. *Electric Power Systems Research*, 114, pp. 1–9. Available: https://doi.org/10.1016/j.epsr.2014.03.031

[3] A. Choudhary, D. Goyal, S. L. Shimi, and A. Akula. (2019). Condition Monitoring and Fault Diagnosis of Induction Motors: A Review. *Archives of Computational Methods in Engineering*, 26(4), pp. 1221–1238. Available: https://doi.org/10.1007/s11831-018-9286-z

[4] F. Jeffali, A. Ouariach, A. el Kihel, and A. Nougaoui. (2019). Infrared thermography based diagnosis of the impact on the kinematic chain. *Proceedings of Materials Today*, 13, pp. 949–955. Available: https://doi.org/10.1016/j.matpr.2019.04.059

[5] J. E. Garcia-Bracamonte, J. M. Ramirez-Cortes, J. de Jesus Rangel-Magdaleno, P. Gomez-Gil, H. Peregrina-Barreto and V. Alarcon-Aquino. (2019). An Approach on MCSA-Based Fault Detection Using Independent Component Analysis and Neural Networks. *IEEE Transactions on Instrumentation and Measurement*, vol. 68, no. 5, pp. 1353-1361. Available: https://doi.org/10.1109/TIM.2019.2900143

[6] W. Dehina, M. Boumehraz, F. Kratz and J. Fantini. (2019). Diagnosis and Comparison between Stator Current Analysis and Vibration Analysis of Static Eccentricity Faults in The Induction Motor. *2019 4th International Conference on Power Electronics and their Applications (ICPEA)*, pp. 1-4, Available: https://doi.org/10.1109/ICPEA1.2019.8911193

[7] Y. Shi, A. Deng, M. Deng, J. Zhu, Y. Liu and Q. Cheng. (2020). Enhanced Lightweight Multiscale Convolutional Neural Network for Rolling Bearing Fault Diagnosis. *IEEE Access*, vol. 8, pp. 217723-217734, Available: https://doi.org/10.1109/ACCESS.2020.3041735

[8] J. Yu, T. Hu and H. Liu. (2019). A New Morphological Filter for Fault Feature Extraction of Vibration Signals. *IEEE Access*, vol. 7, pp. 53743-53753, 2019, Available: https://doi.org/10.1109/ACCESS.2019.2912898

[9] O. E. Hassan, M. Amer, A. K. Abdelsalam, and B. W. Williams. (2018). Induction motor broken rotor bar fault detection techniques based on fault signature analysis – A review. *IET Electric Power Applications*, 12(7), pp. 895–907. Available: https://doi.org/10.1049/iet-epa.2018.0054

[10] M. Delgado-Prieto, J. A. Carino-Corrales, J. J. Saucedo-Dorantes, R. de Jesus Romero-Troncoso and R. A. Osornio-Rios. (2018). Thermography-Based Methodology for Multifault Diagnosis on Kinematic Chain. *IEEE Transactions on Industrial Informatics*, vol. 14, no. 12, pp. 5553-5562. Available: https://doi.org/10.1109/TII.2018.2816925

[11] K. Lang, A. Muetze, R. Bauer and S. Pircher. (2016). Comparison of Induction and Synchronous Reluctance Machine Based Actuators for Elevated Temperature Environments. *IEEE Transactions on Energy Conversion*, vol. 31, no. 3, pp. 1012-1022, https://doi.org/10.1109/TEC.2016.2556716

[12] R. R. Kumar, G. Cirrincione, M. Cirrincione, A. Tortella and M. Andriollo. (2021). Induction Machine Fault Detection and Classification Using Non-Parametric, Statistical-Frequency Features and Shallow Neural Networks. *IEEE Transactions on Energy Conversion*, vol. 36, no. 2, pp. 1070-1080, https://doi.org/10.1109/TEC.2020.3032532

[13] A. G. Garcia-Ramirez, L. A. Morales-Hernandez, R. A. Osornio-Rios, J. P. Benitez-Rangel, A. Garcia-Perez, R. J. Romero-Troncoso. (2014). Fault detection in induction motors and the impact on the kinematic chain through thermographic analysis. *Electric Power Systems Research*, Volume 114, 2014, pp. 1-9, Available: https://doi.org/10.1016/j.epsr.2014.03.031

[14] H. Zhiyi, S. Haidong, Z. Xiang, Y. Yu, and C. Junsheng. (2020). An intelligent fault diagnosis method for rotor-bearing system using small labeled infrared thermal images and enhanced CNN transferred from CAE, *Advanced Engineering Informatics*, vol. 46, 101150, https://doi.org/10.1016/j.aei.2020.101150

[15] A. Choudhary, T. Mian, and S. Fatima. (2021). Convolutional neural network based bearing fault diagnosis of rotating machine using thermal images. *Measurement*, vol. 176, 109196, https://doi.org/10.1016/j.measurement.2021.109196

[16] H. Shao, M. Xia, G. Han, Y. Zhang, and J. Wan. (2021). Intelligent Fault Diagnosis of Rotor-Bearing System Under Varying Working Conditions With Modified Transfer Convolutional Neural Network and Thermal Images. *IEEE Transactions on Industrial Informatics*, vol. 17, no. 5, pp. 3488-3496, https://doi.org/10.1109/TII.2020.3005965

[17] T. Mian, A. Choudhary, and S. Fatima. (2021). A sensor fusion based approach for bearing fault diagnosis of rotating machine. *Proceedings of the Institution of Mechanical Engineers, Part O: Journal of Risk and Reliability*. https://doi.org/10.1177/1748006X211044843

[18] Y. Li, X. Wang, S. Si, and X. Du. (2019). A New Intelligent Fault Diagnosis Method of Rotating Machinery under Varying-Speed Conditions Using Infrared Thermography. *Complexity*. vol. 2019. https://doi.org/10.1155/2019/2619252

[19] A. Choudhary, D. Goyal, and S. S. Letha. (2021). Infrared Thermography-Based Fault Diagnosis of Induction Motor Bearings Using Machine Learning. *IEEE Sensors Journal*, vol. 21, no. 2, pp. 1727-1734, https://doi.org/10.1109/JSEN.2020.3015868

[20] A. Nasiri, A. Taheri-Garavand, M. Omid, and G. M. Carlomagno. (2019). Intelligent fault diagnosis of cooling radiator based on deep learning analysis of infrared thermal images. *Applied Thermal Engineering*, vol. 163, 114410, https://doi.org/10.1016/j.applthermaleng.2019.114410

[21] R. A. Osornio-Rios, J. A. Antonino-Daviu and R. J. Romero-Troncoso. (2019). Recent Industrial Applications of Infrared Thermography: A Review. *IEEE Transactions on Industrial Informatics*, vol. 15, no. 2, pp. 615-625, Available: https://doi.org/10.1109/TII.2018.2884738

[22] G. Singh, T. C. A. Kumar, and V. N. A. Naikan. (2016). Fault diagnosis of induction motor cooling system using infrared thermography. 2016 *IEEE 6th International Conference on Power Systems*, *ICPS 2016*, pp. Available: 11–14. https://doi.org/10.1109/ICPES.2016.7584040

[23] A. Glowacz. (2021). Fault diagnosis of electric impact drills using thermal imaging. *Measurement*, vol. 171, 2021, 108815. Available: https://doi.org/10.1016/j.measurement.2020.108815

[24] D. Lopez-Perez and J. Antonino-Daviu. (2016). Application of infrared thermography to fault detection in industrial induction motors: Case stories. *Proceedings - 2016 22nd International Conference on Electrical Machines*, *ICEM 2016*, pp. 2172–2177. Available: https://doi.org/10.1109/ICELMACH.2016.7732823

[25] E. Resendiz-Ochoa, R. A. Osornio-Rios, Benitez-Rangel, J. P., Romero-Troncoso, R. D. J., & Morales-Hernandez, L. A. (2018). Induction Motor Failure Analysis: An Automatic Methodology Based on Infrared Imaging. *IEEE Access*, 6, 76993–77003. https://doi.org/10.1109/ACCESS.2018.2883988

[26] M. Najafi, Y. Baleghi, S. A. Gholamian, and S. M. Mirimani. (2020). Fault diagnosis of electrical equipment through thermal imaging and interpretable machine learning applied on a newly-introduced dataset. *6th Iranian Conference on Signal Processing and Intelligent Systems*, *ICSPIS 2020*, pp. 1–7. Available: https://doi.org/10.1109/ICSPIS51611.2020.9349599

[27] A. Choudhary, D. Goyal, and S. S. Letha. (2021). Infrared thermography-based fault diagnosis of induction motor bearings using machine learning. *IEEE Sensors Journal*, 21(2), pp. 1727–1734. Available: https://doi.org/10.1109/JSEN.2020.3015868

[28] P. Karvelis, G. Georgoulas, C. D. Stylios, I. P. Tsoumas, J. A. Antonino-Daviu, M. J. P. Rodenas, and V. Climente-Alarcon. (2014). An automated thermographic image segmentation method for induction motor fault diagnosis. *Industrial Electronics Conference*, *IECON Proceedings*, pp. 3396–3402. Available: https://doi.org/10.1109/IECON.2014.7049001

[29] M. Khanjani and M. Ezoji. (2021). Electrical fault detection in three-phase induction motor using deep network-based features of thermograms, *Measurement*, vol. 173, 2021, 108622, Available: https://doi.org/10.1016/j.measurement.2020.108622

[30] Otsu, N. (1979). A threshold selection method from gray-level histograms. *IEEE transactions on systems, man, and cybernetics*, 9(1), 62-66.

[31] Lowe, D. G. (2004). Distinctive image features from scale-invariant keypoints. *International Journal of Computer Vision*, 60(2), 91–110.

[32] Karvelis, P., Georgoulas, G., Stylios, C. D., Tsoumas, I. P., Antonino- Daviu, J. A., Rodenas, M. J. P., and Climente-Alarcon, V. (2014). An automated thermographic image segmentation method for induction motor fault diagnosis. *IECON Proceedings (Industrial Electronics Conference)*, 3396–3402.

[33] Tran, V. T., Yang, B. S., Gu, F., and Ball, A. (2013). Thermal image enhancement using bi-dimensional empirical mode decomposition in combination with relevance vector machine for rotating machinery fault diagnosis. *Mechanical Systems and Signal Processing*, 38(2), 601–614.

[34] Kurita T. (2020) Principal Component Analysis (PCA). In: Ikeuchi K. (eds) Computer Vision. Springer, Cham.

[35] Boehmke, B. and Greenwell, B. (2019). Hands-On Machine Learning with R. CRCPress.